Review article

Eric Audouard*, Guillaume Bonamis, Clemens Hönninger and Eric Mottay

GHz femtosecond processing with agile high-power laser

High power and flexible fs lasers in GHz burst mode open new horizons for femtosecond laser processing

https://doi.org/10.1515/aot-2021-0029
Received May 31, 2021; accepted August 9, 2021;
published online September 3, 2021

Abstract: Bursts of GHz repetition rate pulses can significantly improve the ablation efficiency of femtosecond lasers. Depending on the process conditions, thermal mechanisms can be promoted and controlled. GHz ablation therefore combines thermal and non-thermal ablation mechanisms. With an optimal choice of the burst duration, the non-thermal ablation can be highly enhanced by a heating phase due to the first pulses in the burst. The GHz burst mode can be considered as a key function for the "agility" of new high-power lasers.

Keywords: femtosecond laser; femtosecond processing; GHz bursts; temporal pulses shaping.

1 Introduction

One of the most striking points, when considering the femtosecond laser applications field, is the very large number and wide variety of possible applications. Such a situation is a direct consequence of the original physical nature associated with the laser matter interaction in the femtosecond regime. Allowing the creation of temporary states of matter far from equilibrium, where the temperature of the atomic lattice is no longer directly related to the temperature of the electrons, the nature of the ablation in the femtosecond regime is therefore very different from other lasers. All materials, from the most fragile to the hardest, can be treated. In all cases there is a considerable reduction in the heat affected zone (HAZ), i.e. the area modified by thermal diffusion, outside the area irradiated by the laser. This characteristic of the interaction leads to the greatest precision of treatment reachable with a laser [1–3].

Over the past 10 years, femtosecond laser processing applications have seen a tremendous development. The ability of femtosecond lasers to offer a very precise, high quality laser ablation combined with the average power increase enables higher and higher industrial throughput, in turn opening new applications.

Femtosecond laser applications have been enabled by a continuous and rapid increase of the lasers average power over two decades, as illustrated in Figure 1. The current state of the art for industrial applications is 50–300 W, with kW average powers having been demonstrated in several laboratories worldwide [4] and being actively developed to industrial maturity.

Amplitude has developed a hybrid fiber/crystal concept [5] enabling both short pulse duration and high pulse energy. Moreover, this concept facilitates the implementation of fully user controllable pulse repetition rates. The laser architecture consists of a fiber-based seed module with a 40 MHz broadband passively mode-locked oscillator, a pulse picker, and several fiber amplifiers (Figure 2). The wide gain bandwidth of Yb-doped fibers is the key to the generation of short femtosecond pulses. In standard operation, the laser source allows pulse-to-pulse picking and modulation of the amplified pulse train up to 2 MHz by using the external modulator.

The scaling to high powers and high pulse energies, and ultimately to the kW level, is accessible thanks to the choice of crystal-based laser amplifiers with high gain and superior thermal management. Figure 3 shows the efficient power extraction curve of a fiber-/crystal femtosecond amplifier up to kW average power: 1210 W, 1.2 mJ at 1 MHz (before pulse compression). The spectral Bandwidth is 1.7 nm and the pulses can be compressed to 600 fs ($sech^2$).

***Corresponding author: Eric Audouard**, Amplitude Laser Group, 11 Avenue de Canteranne, Cité de la Photonique, 6 allées des Lumières, Bâtiment MEROPA, Pessac, 33600, France,
E-mail: eric.audouard@amplitude-laser.com
Guillaume Bonamis, Clemens Hönninger and Eric Mottay, Amplitude Laser Group, 11 Avenue de Canteranne, Cité de la Photonique, 6 allées des Lumières, Bâtiment MEROPA, Pessac, 33600, France

Figure 1: Average power increase for AMPLITUDE lasers. ×1000 in 20 years.

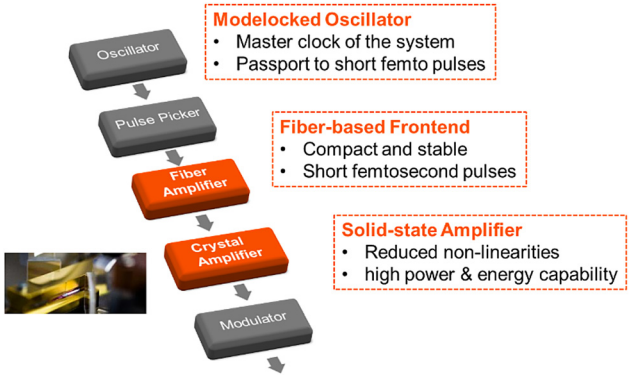

Figure 2: Linear architecture of AMPLITUDE high power femtosecond lasers.

Making use of the available high average power for new applications of femtosecond will require new laser functions. Coupling a high-power laser with advanced beam engineering techniques will result also in an agility which is key for process development. Figure 4 shows several "agility" options today available for fs lasers. Fs pulses are generated by the laser source at a given energy and repetition rate. Pulse shaping can adjust the pulse train by creating bursts of pulses at different intra burst repetition rate, that can be also shaped in amplitude. Pulse repetition rate can be rapidly changed with high precision triggering. Pulses with different pulse duration can be also generated and superimposed. Additional optical modules can spatially shape the laser beam, and pulses compression techniques can reduce the pulse duration down to several tens of femtoseconds.

In this frame, higher ablation efficiency may be a key advantage. As shown in Figure 4, femtosecond lasers can be operated in a mode delivering single pulses temporally divided in trains of high-repetition rate pulses, called bursts. The pulses have an energy corresponding to the single-pulse energy divided by the number of pulses within the burst. The fluence of each pulse of the burst can be adjusted close to the optimal fluence, defined as the fluence at which the ablation rate is the highest [6]. An increased ablation volume per pulse has been reported [7–9] but not exceeding a 10–30% increase compared to single-pulse ablation. In such configurations, the choice of the laser parameters (number of pulses per burst, delay between pulses in the burst, fluence per pulse) will strongly influence the efficiency of the process. In addition, thermal accumulation can occur deteriorating the machining quality, and a plasma shielding effect can decrease the pulse absorption and the efficiency of the laser process [10].

GHz-bursts, i.e. pulse trains of femtosecond pulses with repetition rates in the GHz range within the pulse train, have shown promising results for material processing, featuring very high ablation rates. Early publications have shown that ablation in the GHz regime increases the

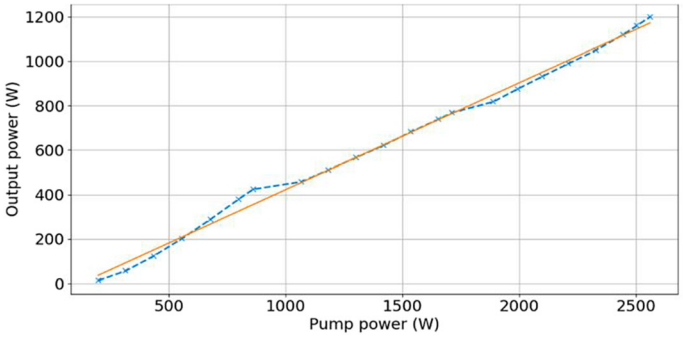

Figure 3: kW fs laser at AMPLITUDE.

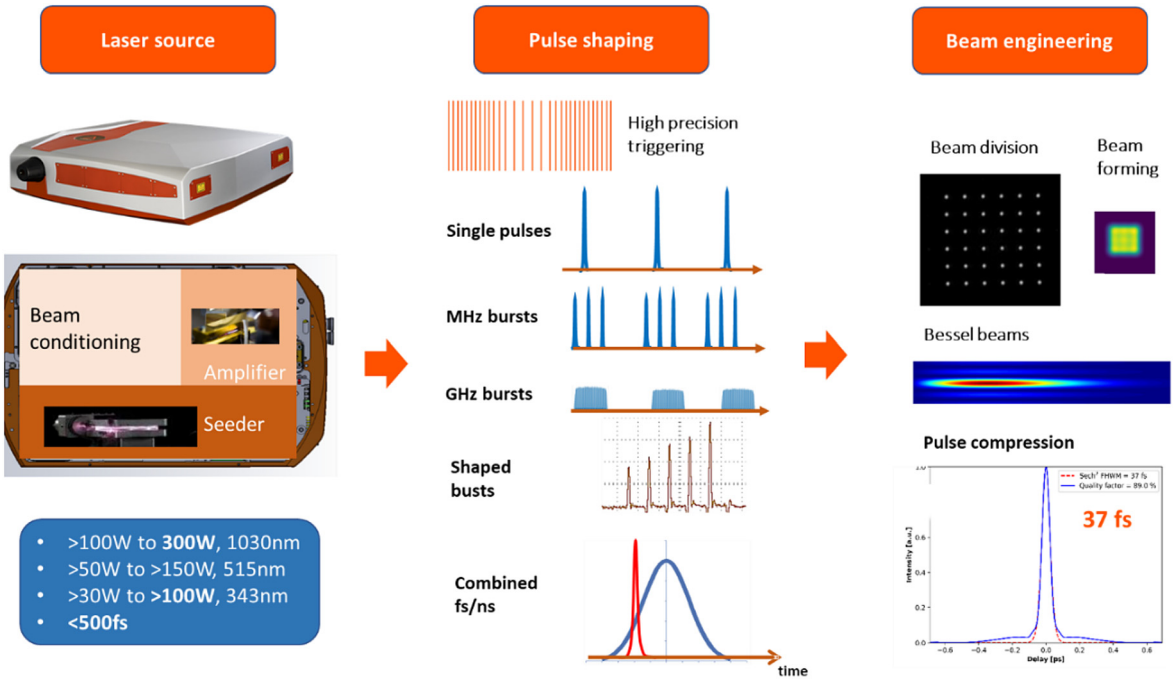

Figure 4: «Agile» femtosecond lasers: possible functionalization of the laser pulses and pulses beam.

ablation efficiencies by an order of magnitude [11, 12]. The GHz ablation mechanisms are a combination of thermal and non-thermal ablation mechanisms, each dominating at specific burst parameters and laser fluences. Determining the optimum laser and process parameters is therefore not straightforward. Nevertheless, studies made on a wide range of parameters have shown that a rather simple interpretation of GHz ablation can be given [13]. Indeed, as shown by systematic studies [14] the results depend strongly on the applied laser parameters and understanding the ablation mechanisms is required to optimize the process.

In this paper, we present the GHz burst mode as an element of agility of great interest for femtosecond laser applications. While the contribution of thermal effects may make it more difficult to achieve optimal quality, controlling these thermal effects can also pave the way for new and very original applications.

2 Burst of pulses

The term "burst" is here used for a train of N pulses separated by typically one oscillator period (25 ns for a 40-MHz oscillator, 1 ns for a 1-GHz oscillator). In the case of the laser architecture presented above the bursts are generated using the pulse picker (Figure 2). Laser-matter interaction using bursts has been extensively studied [7, 15, 16]. The role of pulse-to-pulse thermal accumulation has been widely demonstrated, as a phenomenon either beneficial when increasing the ablation efficiency or detrimental when degrading the machining quality due to thermal effects. Additional potentially detrimental mechanisms, such as shielding effects or the surface roughness increase have been reported [6, 10].

If we do not consider these limiting mechanisms, the ablation rate can be estimated using simple models based on analytical calculations [17]. For a burst composed of N pulses with the same energy Ep, and a burst repetition rate f, the ablation rates D and ablation efficiency $e = D/P$ is given by:

$$D = Nfk\ln^2 F \tag{1}$$

$$e = Nf\frac{k}{P}\ln^2 F = \frac{k}{Ep}\ln^2 F \tag{2}$$

In this approach, two fitted parameters δ and Fth describe the material, Fp is the fluence of a single pulse and $Ep = \pi w_0^2 Fp$ its energy. In eqs. (1) and (2) $k = \frac{\pi w_0^2 \delta}{4}$ and $F = \frac{2Fp}{Fth}$.

Equation (1) shows that the ablation rate can be increased by the number of pulses in the burst N but the efficiency is independent of N.

Equation (2) underlines a burst specific behavior in the case of a burst with a total burst energy equal to the energy

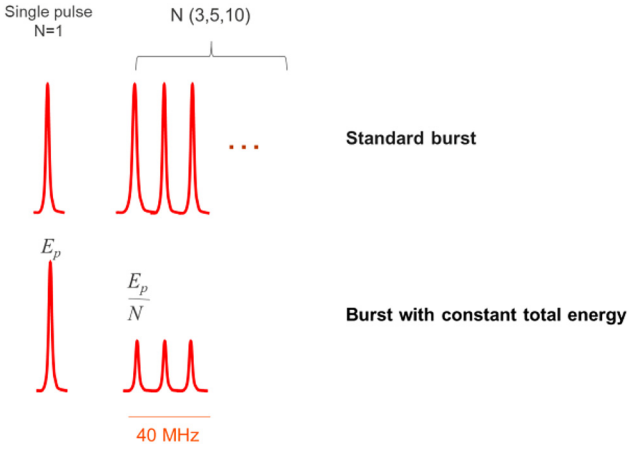

Figure 5: Standard burst configuration compared with burst conserving the total energy of the corresponding single pulse.

of the single pulse (cf. Figure 5). Equation (2) shows a maximum value, obtained for $F_{\text{opt}} = \frac{e^2}{2} Fth$ which indicates an optimal fluence value with a maximum efficiency. Since the threshold fluences of metals are generally quite low, this optimal fluence is therefore also low and indeed rarely used for a process. For stainless steel, we can estimate *Fth* at 0.1 J/cm^2, and the optimal fluence is around 0.5 J/cm^2. The burst will perform more efficient ablation compared with the corresponding high energy single pulse since the sub pulses of the burst can settle in a lower fluence domain where these sub pulses are more efficient.

To evaluate this "efficiency control", let's write eq. (2) in the case of a *N* pulses burst conserving the total energy of the corresponding single pulse, the corresponding fluence of sub pulses is then *F/N*.

$$e = N \cdot f \cdot \frac{k}{P} \ln^2 \frac{F}{N} = \frac{\delta}{2Fth} \cdot \frac{N}{F} \ln^2 \frac{F}{N} \tag{3}$$

Figure 6 shows results of efficiency calculation for $N = 3, 5, 10$ compared with the single pulse result ($N = 1$). Only the dimensional factor $(N/F)\ln^2(F/N)$ in eq. (3) is represented to evaluate the differences between each case. The represented fluence is the single pulse fluence *Fp*, estimated in the stainless-steel case (the reduced fluence is $F = 2 \cdot Fp/Fth$ with $Fth = 0.1$ J/cm^2). The figure illustrates the predicted behavior: depending on the total burst fluence, the maximum efficiency is the same for each value of *N*. The corresponding fluence for this maximum is slightly shifted toward the higher fluences with the value of *N*. As shown in other works [7], if the different efficiencies are represented in function of the burst pulses fluence *Fp/N*, the results will be superimposed in the same curve. This simple approach gives the general trend of ablation with bursts but does not consider the role of the thermal effects derived for the thermal accumulation mechanism. As already mentioned, these thermal effects can have a significative contribution to ablation, and this is always true in the case of GHz pulses as we will see in the following section.

3 GHz burst of pulses

Considering laser high repetition rates, the ablation with fs pulses involves also thermal mechanisms, previously considered as having low influence on femtosecond processing. Beyond several hundred kHz, the delay between the laser pulses is usually less than the material thermal relaxation time and there is thermal accumulation in the target material. The resulting rise in temperature introduces changes in morphology and surface chemistry [18, 19], at the expense of machining quality [2]. The corresponding thermal effect on the whole ablation process depends on the delay between the pulses compared to the lifetime of the thermal mechanisms involved. If the delay between the pulses is less than this lifetime, each pulse therefore sees a thermally modified material. In this context, the burst mode can be identified as a method increasing the repetition rate only during the burst train, allowing control of the thermal effects generated by thermal accumulation [20]. Bursts with a user defined number of pulses and shapes over a wide range may be advantageous and promote the burst mode as a key contribution for laser agility. The use of higher numbers of sub pulses in burst trains with a period down to the nanosecond or picosecond range, corresponding to GHz repetition rate, have shown a potentially significant high increase of ablation efficiency in the first published works [11, 21, 22]. Thermal accumulation, if occurring over the duration of the burst, can induce a material ablation threshold lowering [19, 23]. Such a behavior will benefit the ablation mechanism as we will see in the following.

3.1 GHz laser technology

We present in this section details on recent developments of GHz laser technology. In addition to their application to micro-machining, initially proposed by Kerse et al. [11], GHz ultra-short laser sources are also used in the field of telecommunications [24], spectroscopy in the temporal domain [25] or the generation of polarized electron beams for particle accelerators [26]. Different pathways have been explored to design these lasers. Two main methods can be distinguished: a repetition rate increase from a moderate-repetition rate source (typically in the MHz range) or a

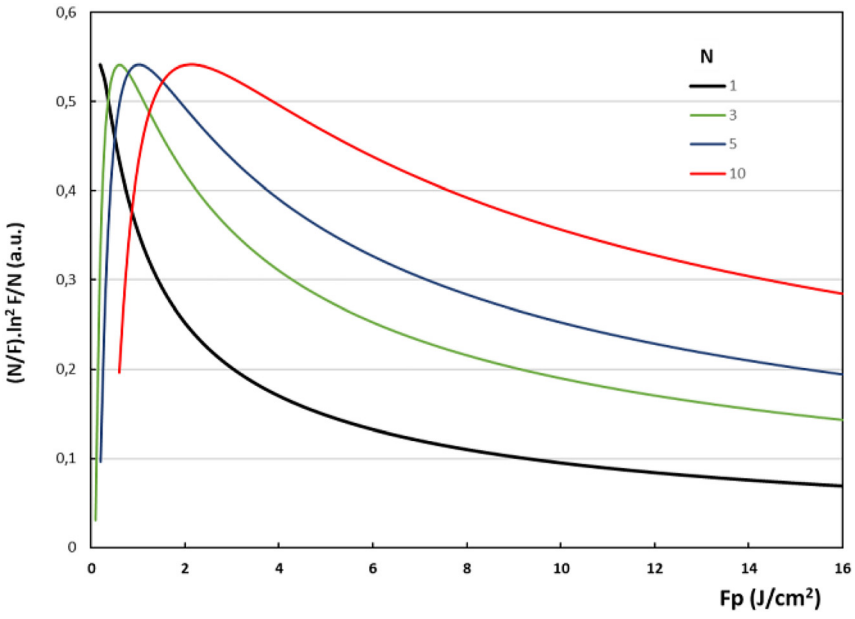

Figure 6: Calculation of efficiency of a single pulse ($N = 1$) and a burst ($N = 3, 5, 10$) of the same total energy.

direct generation of high repetition rate pulses trains. For the first approach, the used technics, such as cascading fiber delay lines, are using a moderate repetition rate femtosecond oscillator [27]. This method however presents several disadvantages: the complexity of the fiber assembly, and its phase influence leading to varying the pulse durations within the GHz burst after compression. The second option is a direct generation of high repetition rate pulses trains, for example using passive mode locking by Kerr effect [28], soliton [29], or other implementations of passive mode locking [30], and finally the modulation of phase and amplitude from a continuous laser diode [31, 32]. These methods avoid the complexity of repetition rate multiplication but create new problems. The oscillator design involves very small cavities (about 10 mm) [29], and techniques using phase and amplitude modulations require the use of complex and expensive components. For the design of a simple and stable laser suited for industrial applications, we opted for a hybrid concept: the design of a mode-locking oscillator at a repetition rate of the order of the GHz and a multiplication of this cadence with additional fiber delay lines. Pulses from the oscillator are then injected into several stages of the amplification, to obtain the average power levels needed to conduct machining experiments.

The laser architecture is basically identical to the one represented in Figure 2 and the functioning scheme is illustrated in Figure 7. The only major modification is the replacement of the 40-MHz oscillator by a GHz oscillator. To access to higher repetition rates with the same oscillator, optional fiber-based delay lines can be introduced to double or quadruple the oscillator pulse repetition rate. Bursts are obtained by picking series of pulses from the original pulse train with an Acousto-Optic Modulator (AOM). Amplification of these bursts would cause an asymmetric energy distribution within the burst due to gain depletion. To compensate for this effect, the AOM is driven by an appropriate amplitude-shaped signal provided by an Arbitrary Waveform Generator. However, the rise and fall-times of the AOM are slow with respect to the GHz repetition rate thus leading to lower energy for the first and last pulses of the burst. These pulses are removed by an Electro-Optic Modulator, presenting short enough rise and fall times. These two components together with the optional delay lines allow to vary the pulse repetition rate, the burst repetition rate, the number of pulses per burst and the energy distribution inside the burst over a wide range.

3.2 GHz ablation

If the fluence of each pulse of the burst is higher than the ablation threshold, the ablation starts from the first pulse and prevent an efficient accumulative heating. Nevertheless, the ablation generates also thermal effects as shown by the obtained experimental results [33, 34]. The ablation process in such conditions is similar or even worse to those occurring in the MHz-burst regime.

If the burst pulses energy and the corresponding fluence is below the ablation threshold, no ablation occurs at

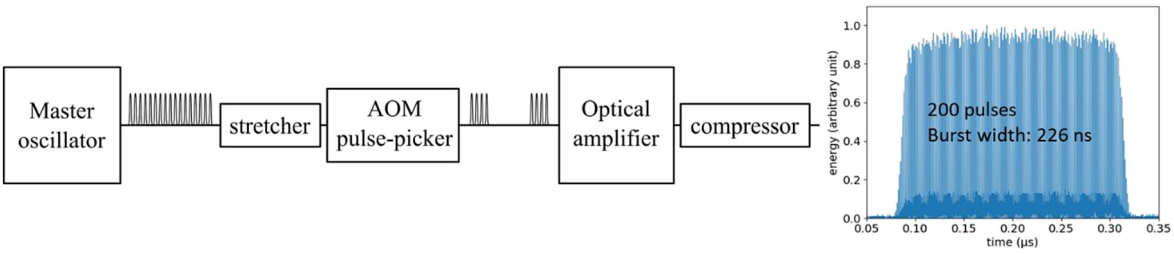

Figure 7: Principle of GHz bursts generation. Burst energy 2 mJ, burst rate: 50 kHz, 200 pulses with 10-µJ pulse energy.

the beginning of the pulses train and the matter is slowly heated by thermal accumulation. The temperature rise then reduces the ablation threshold [37]. If the ablation threshold is reduced close to the pulses fluence value, each subsequent pulse can ablate matter very efficiently, since fs ablation efficiency is optimal when the fluence is just above the ablation threshold. Between the two steps, a very efficient thermal mechanism occurs, and melting material is always seen in GHz ablation as experimentally evidenced [13]. Figure 8 summarize the presented different GHz burst configurations.

The specificity of GHz ablation is highlighted when using a large enough range of laser parameter variations to obtain an optimum result both in ablation efficiency and quality [13]. Silicon is an excellent candidate since fs or ps ablation of silicon has already been the subject of many studies and has also many industrial applications [11, 13, 21, 23, 25]. In Figure 9, the evolution with fluence of the efficiency and the ablated crater morphology [13] is shown. The number of pulses per burst was adjustable using a compact and integrated laser system described in Section 3.1, for 0.88 GHz intra-burst repetition rates, 100 pulses in the burst and a burst repetition rate fixed to 100 kHz.

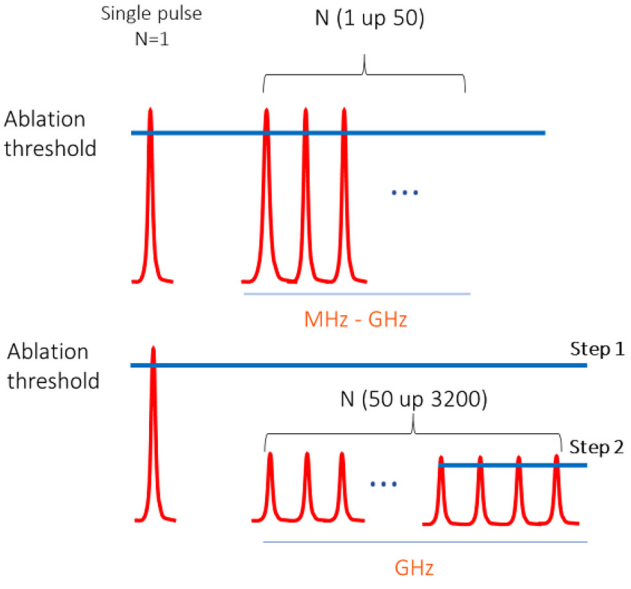

Figure 8: Different GHz and MHz burst configuration.

The ablation morphology shows deep craters with remelting deposits. The amount of redeposited material remains almost constant when the depth of the crater increases with fluence. Two different types of laser modifications are evidenced. Bumps are formed at low fluences, and ablation craters appear at higher fluence, above a crater threshold *Fc*. The bumps are usually elevated in the center by few hundred nanometers and surrounded by depressed areas. This results from the expansion of the silicon during the fusion [36] and is the signature of this heating phase. The craters are surrounded by a splash of molten material near the crater threshold, but the splash becomes negligible compared to the volume ablated (less than 3% for a burst energy more than 10 J/cm^2). We note that the crater formed just above the threshold is already deep, with a depth of 2.6 µm.

The fluence threshold *Fc* corresponds to a lattice temperature *Tc*. *Tc* is reached at the end of the heating phase, when each burst pulse contributes to an increase of the lattice temperature. The linear absorption and free-carrier absorption coefficients of silicon are temperature dependent. The ablation threshold for silicon drops with increasing lattice temperature. For example, a decrease from 0.43 to 0.25 J/cm^2 is reported when the temperature is increased from room temperature to 300 °C [37]. At the threshold *Fc* for crater formation, the heating time equals the burst width. The volume thermally affected by the burst will be determined by a characteristic heat diffusion length l_D. Let us consider a common simple calculation for diffusion length l_D: $l_D = \sqrt{Dh \cdot \tau}$ where Dh = 0.86 cm^2/s is the thermal diffusivity coefficient for silicon at room temperature. The obtained l_D value equals 2.9 µm for the 0.88 GHz and 100 pulses. This value follows closely the experimentally measured crater depths (2.6 µm). Once *Tc* is reached, an efficient ablation process starts on the heated remaining layer. The optimal regime is achieved when the depth of this heated layer is comparable to the

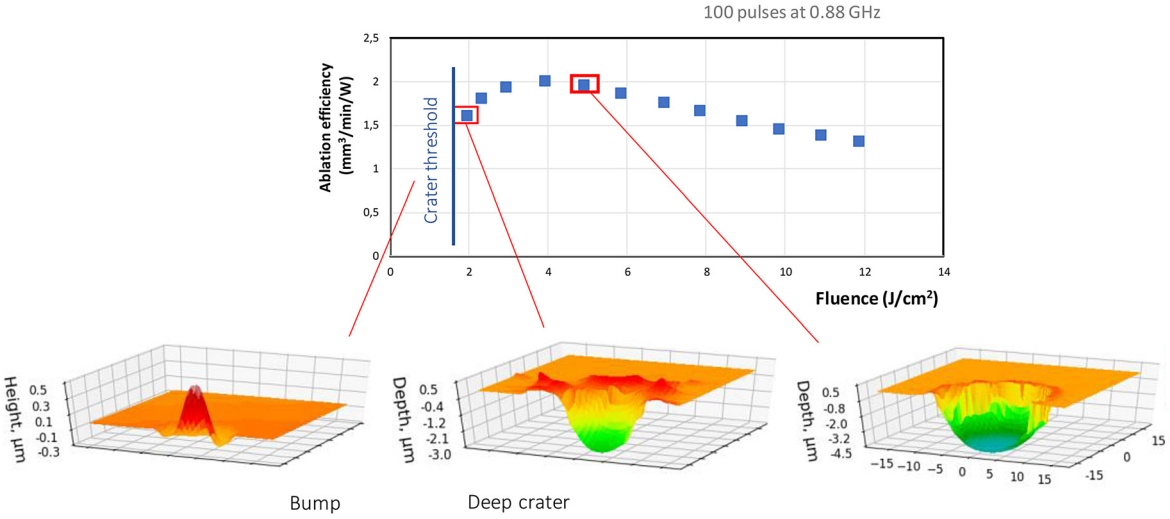

Figure 9: Efficiency and morphology of silicon modification after GHz ablation, experimental conditions: bursts of 100 pulses at 0.88 GHz intra burst repetition rate. 3D reconstructions produced from optical confocal microscopy measurements. Left: bumps few hundreds of nm height, obtained for a fluence higher than 1.2 J/cm^2 up to the crater threshold. Middle: the crater near the threshold of 1.8 J/cm^2 right: deeper crater with higher fluence. Results are taken from ref. [13].

ablation depth of a single pulse. For example, at 3.52 GHz for Dh = 0.12 cm^2/s, the corresponding heat diffusion length is estimated as 60 nm at about 1400 °C [38], which is close to the average affected depth by a single fs pulse in silicon (~40 nm) [39].

The above presented simple physical approach in two steps, summarized in Figure 10 can lead to the determination of the optimal laser parameters. The burst fluence threshold has to be estimated for a given material, and the minimal burst length deduced. Then an optimal fluence and an optimal number of pulses can be estimated to maximize the "non-thermally" ablated volume versus the thermally ablated volume. An iterative method is thus possible to estimate the best laser parameters for a given experimental configuration [40].

A more detailed understanding of the physical mechanisms involved in GHz ablation is still needed. A theoretical description of the nature and characteristic times of thermal mechanisms involved are required to clarify the highlighted thermal effects. Early results have been obtained using a numerical model constructed to simulate the macroscopic surface heating mechanism in femtosecond laser processing [41]. First results using a 1D hydrodynamic model brings information on the physical scenario, showing that the "traditional" quasi-isochoric heating shown by thermodynamic paths after single pulse interaction is replaced by an isobaric process with oscillations around the binodal [42].

3.3 Process influence

The above schematic description highlights the existence of a highly efficient thermal mechanism occurring when a threshold is reached by thermal accumulation, in a volume related to the thermal diffusion length l_D. This mechanism will be sensitive to the sample volume addressed by the process and may therefore have a different efficiency if a crater, a line or a cavity is generated. For instance, for a crater formation, the irradiated material is confined during the process, meanwhile, for line engraving, the involved volume depends on the relative movement of the sample and the beam. The GHz ablation results are thus expected to depend on the selected process. It can be surprising since it was not the case for a single pulse ablation that shows no efficiency difference between different type of processes: drilling (crater formation), cutting (line engraving), or milling (cavity formation).

Figure 11 presents a comparison of ablation efficiencies for crater formation, line scribing and cavity milling in copper [43]. Other results can be found in ref. [14]. Experiments have been performed for different burst durations, total burst fluences, intra-burst repetition rates and number of pulses within the burst, in the case of an intra-burst repetition rate of 0.88 GHz and 200 pulses per burst (corresponding to a total burst duration of 226 ns). The burst-to-burst overlap was fixed at 48% for both line scribing and cavity milling. The specific ablation rates

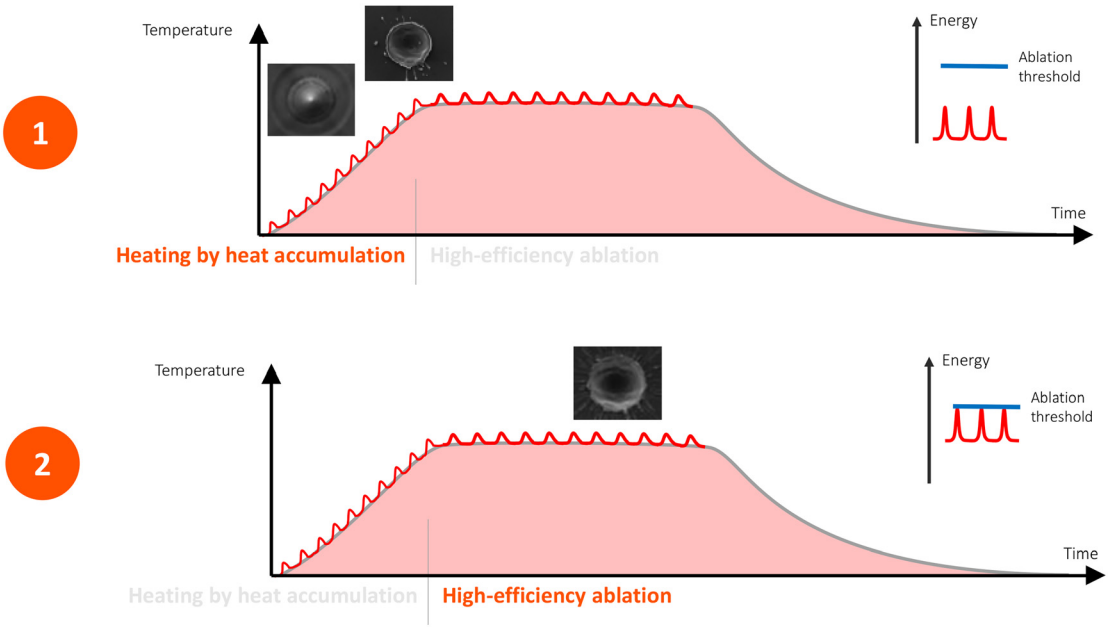

Figure 10: Schematic description of the two steps GHz ablation mechanism. SEM images are from ref. [13].

show the highest values for crater formation (circles) which are slightly exceeding the ones for line scribing (lines), whereas the ones for cavity milling (squares) have lower values. As expected, a difference exists between the three processes, but remains weak.

Because of the role played by thermal effects, the increase of ablation efficiency in GHz ablation can lead to a degradation in quality. As shown in ref. [14], a quality evaluation is possible, depending on the selected process.

In the case of line engraving, the ablated volume and the volume of recast material above the surface at the machining edge is measured. A quality factor is then determined by the ratio of the two volumes and expressed as a percentage. This quality factor is of course obtained for a set of fixed parameters, scan speed (or pulses overlap), number of pulses in the burst. As might be expected, the increase in efficiency goes hand in hand with an increase in the quality of machining. The longest bursts present the highest ablated matter sections and lowest redeposited matter corresponding to the highest Q factor. In the range of the tested burst fluences between 7 and 83 J/cm^2, the Q factor stays nearly constant. Consequently, for line scribing

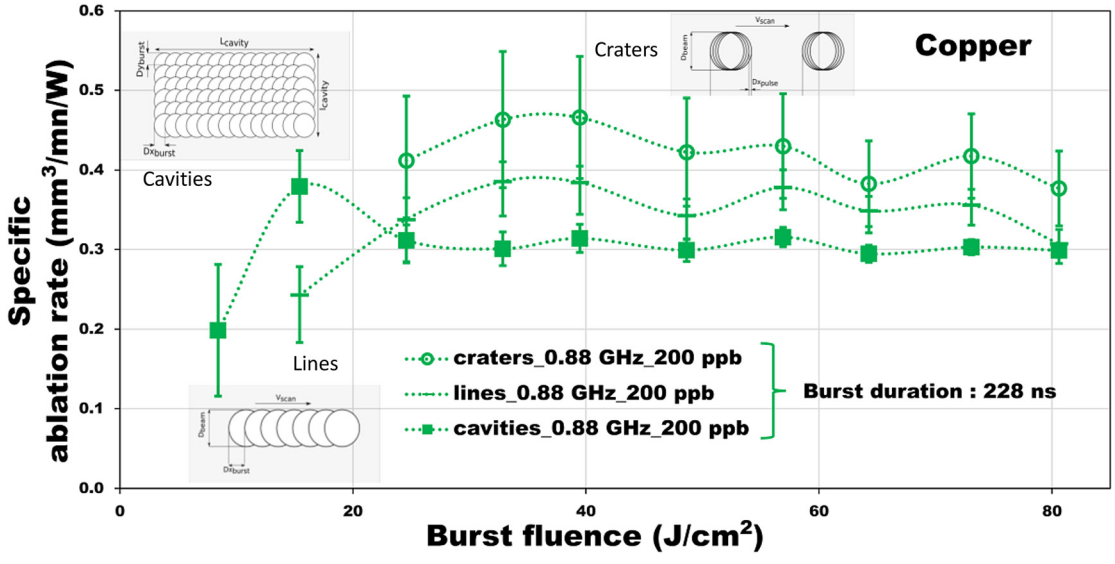

Figure 11: In the case of copper, comparison of ablation efficiency for different usual processes: drilling, cutting and milling, from ref. [43].

the ablation efficiency and the quality factor can be controlled over a wide range of fluences by adjusting the burst duration.

For cavity formation, the surface rugosity can be measured by confocal microscopy [14]. The roughness of the cavity bottom surface is strongly increasing with the burst fluence, especially for aluminum (from a *Sa* roughness of 1.32 µm at 7.0 J/cm^2 to 5.49 µm at 37.5 J/cm^2). Copper is the only tested material presenting a *Sa* roughness below 1.0 µm up to 37.5 J/cm^2. The roughness obtained for copper are similar to those reported from a femtosecond single-pulse machining [44]. For silicon, lower roughness is observed for single-pulse machining, at slightly lower fluences [6]. It is therefore difficult to combine high ablation efficiencies and low surface roughness for milling with a one-step process. Nevertheless, recent work [45] has shown that the use of GHz bursts with a large number of low-energy pulses allows high-quality polishing, and with greater efficiency than using MHz bursts. Similar results are presented in ref. [46], a two-step ablation process achieve better roughness of the surface irradiated by long bursts: a first stage of GHz moderate-energy ablation and then a polishing stage with the same low-energy GHz burst.

The above presented results of GHz-burst machining for line scribing and cavity milling have been obtained with a fixed burst-to-burst overlap of 48%. Different values show a limited impact on the ablation results [14]. This optimal value is different from the one usually used in fs processing with single pulses (around 70%) [2]. It can be interpreted as the result of thermal accumulation that occurs differently during GHz burst and single pulse machining. In the conventional single-pulse ablation regime, a variation in spatial overlap causes thermal accumulation in the material, depending on the repetition rate [2]. When the overlap is too low, there is no thermal build-up. Intermediate overlap allows to benefit from thermal accumulation that increases ablation; and damaging thermal effects appear with high spatial overlap (uncontrolled melt bath, burrs). In the GHz burst ablation regime, thermal accumulation already occurs during the burst and increases with its duration as previously shown. The effect of spatial overlap on thermal accumulation are thus limited for short bursts. It makes critical the use of high overlaps with long bursts. Therefore, the use of a lower spatial overlap than for single-pulse machining should be preferred for GHz burst machining (close to 50% rather than 70%). This influence of the overlap on the ablation rate and machining quality underlines also the specificity of GHz-bursts with respect to single-pulse processing.

Also notice that, because of evidenced thermal heating, GHz ablation on dielectrics materials give good results only in some specific cases [35]. The generation of micro cracks because of this confined heating has to be avoided or controlled.

3.4 Ablation efficiency results

As shown in the previous section, the GHz ablation efficiency will depend on the selected process and experimental configuration. The highest ablation efficiency is obtained for crater formations [13], 200 pulses at 0.88 GHz and a spot size of 24 µm resulting in a total burst fluence of 6.8 J/cm^2. Such conditions lead to a specific removal rate of 2.5 mm^3/min/W, that is the highest so far reported GHz ablation efficiencies. This maximum value depends on the experimental set up, and more precisely on the laser spot size on the sample. For the same experiment but with 24 µm spot size [14], a maximal specific ablation rate of 1.6 mm^3/min/W is observed, 37% lower than in ref. [13].

Therefore, comparison of experimental results has to be handled with care. As a first condition, results for the same type of process can be more safely compared. The benefits of using GHz bursts of femtosecond pulses are today discussed, both in terms of quality and efficiency obtained in comparison to standard machining by femtosecond pulses, bursts of lower rates (MHz) or nanosecond pulses. Table 1 brings together specific ablation rates achieved in the literature for silicon, copper and steel with four different laser configurations: single-pulse machining, femtosecond and nanosecond, MHz bursts and GHz bursts. All these results are achieved by milling cavities. Compared to single femtosecond pulses, GHz bursts are significantly more efficient only for large burst durations. For example, for copper, GHz bursts of 57 ns [14] and 4.6 ns [33] have lower ablation rates than conventional femtosecond machining [20, 33]. The interest of the GHz bursts appears only for bursts of 228 and 912 ns. This observation is also true when comparing the ablation rates of GHz bursts with nanosecond pulses or MHz bursts: there is a burst-time threshold beyond which GHz burst machining becomes more interesting than other machining processes to increase ablation efficiency.

In the case of cavities preformed in stainless steel, a detailed comparison of results obtained for maximum achievable energy specific volumes is presented in a recent review paper on metals ablation with burst pulses [47]. Figure 12 of this paper is reported in the following figure. The role of burst duration on ablation efficiency is also underlined.

Table 1: Comparison of maximal specific ablation rates (in $mm^3/min/W$) reached for milling for silicon, copper and Stainless Steel. The values are given for single femtosecond-pulses [20, 33], MHz-bursts [20], GHz-bursts [14] and single nanosecond pulses [20].

Burst duration	Single-pulse mode			Burst mode				
	fs [21] 380 fs	fs [25] 230 fs	ns [21] 175 ns	MHz [21] 175 ns	GHz [25] 4.6 ns	GHz [14]		
						57ns	228 ns	912 ns
Silicon	0.24	0.26	0.72	0.51	0.10	0.58	1.26	1.44
Copper	0.18	0.19	0.40	0.25	0.02	0.16	0.38	0.66
Steel	0.24	0.29	0.20	0.15	0.02	0.10	0.30	0.67

GHz fs ablation is reaching the ns pulses ablation efficiency. As discussed in ref. [47] and in ref. [14] the remaining work to do is a confrontation of the obtained quality in ns pulses and GHz fs bursts ablation. Obviously, GHz fs bursts offer more flexibility to control ablation quality than ns pulses.

To give another view of possible results, Figure 13 compares several better ablation efficiency results obtained for line engraving in the case of copper. The better GHz results [43] is still obtained for the longer bursts: 912 ns (1600 pulses at 1.76 GHz). It is compared with MHz bursts [9] and single pulses efficiency [3].

3.5 Thermal treatment with GHz pulses

The previous discussion on surface roughness have underlined potential new perspectives for fs GHz lasers, based on thermal modification for surface polishing [45, 46]. Other applications can emerge from this new possibility to use controlled thermal modification of materials. The rationale for femtosecond pulses (from 100 fs to 1 ps) is to perform very localized material modifications, typically on an area comparable to the spot size on the sample (typically from 20 to 40 µm in diameter). The material outside the area under irradiation is usually affected over a very small distance (1–3 µm). Among all the lasers used in industry, femtosecond lasers generate the smallest thermally affected zones, which motivates their use for welding implemented at micron or sub-micron scales. This unique ability expands the field of welding to smaller welding-scales still unexplored. The nature and morphology of the intra volume modification depend on the pulse energy but also on the pulse-repetition rate and the light propagation in the materials. Although the behavior of a weld involving metals is different from the glass-to-glass case, the heating by thermal accumulation must be considered in both cases.

The first results of glass/glass welding by fs pulses were published around 15 years ago [48] and have

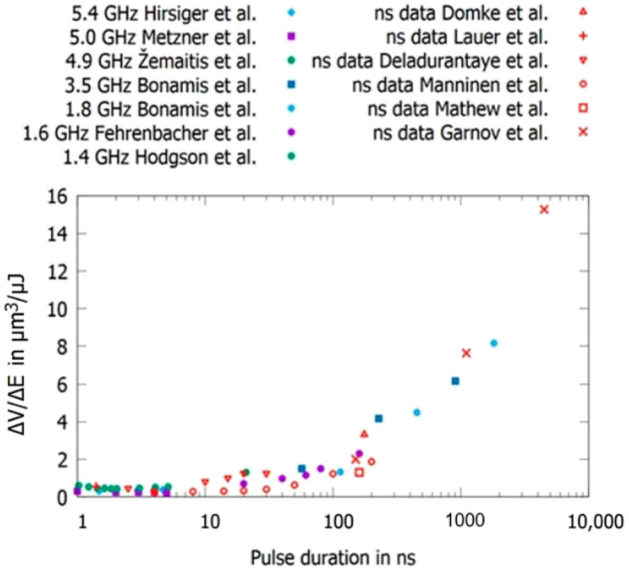

Figure 12: From Ref. [47] (Figure 12), maximum achievable energy specific volumes (in $\mu m^3/\mu J$) for milling in stainless steel, in function of the GHz burst duration. Results obtained with ns pulses are also shown.

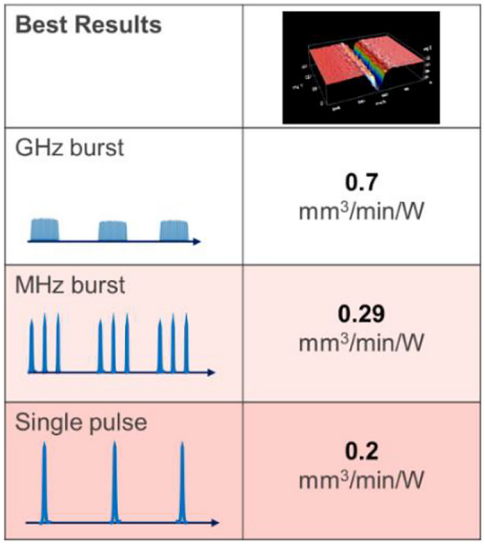

Figure 13: Best results for ablation efficiency of copper by GHz busts [43] compared with MHz bursts [9] and single pulses [3] for lines engraving.

pioneered new ideas on the use of femtosecond pulses for welding transparent materials. A few years later, the first glass/copper welding [49] has been addressed and more recently the first results have been obtained on ceramics [50], and for semiconductor-metal welding [51].

A quite new approach could involve the thermal control associated with GHz burst mode, in the first heating phase. As said above, this heating time can be controlled by the number of pulses in the burst and thus, the heating can be precisely controlled by the number of pulses in the burst.

4 Conclusions and perspectives

This review of fs GHz bursts of pulses underlines their potential higher ablation efficiency compared to standard femtosecond pulse ablation regimes. Optimal ablation with GHz bursts implies a final adjustment of a wide range of laser parameters, explaining the variety of conclusions that could be drawn from various work on GHz ablation, performed with different laser parameters. The key parameter for GHz ablation is the burst duration and the corresponding number of pulses in the burst. The adjustment of this duration will lead to an optimal compromise between the ablation efficiency and the quality of the machining process. The optimal number of pulses, at a given intra-burst GHz repetition rate can be found to maximize the volume of ablated material and minimize the redeposited material.

New perspectives are open to laser processing with fs GHz lasers, based on thermal modification, such as welding of all materials (metals, ceramics, dissimilar materials) or surface polishing. A laser developed on a flexible industrial laser basis (up to 300 W in IR, 100 W in UV), energy-shaped bursts for a high number of pulses can be used to increase the panel of laser applications open to femtosecond processing.

New applications of high average power femtosecond lasers for high precision manufacturing present specific challenges. The thermal management of the beam on the workpiece, which was a minor subject when using low or medium average power lasers, is now of the upmost importance. Temporal and spatial shaping, amplitude and phase control, precise temporal synchronization, fiber delivery, which have been demonstrated at the laboratory level will see increasing use in real life applications. Moreover, digital processing, machine learning and the flexibility enabled by the 4.0 industry framework will also be key sources of innovation.

Fs GHz high power lasers have to be considered in the more general frame of the average power increase of femtosecond lasers, going hand in hand with their agility to make efficient the available Watts. The productivity increase thus possible will of course affect all existing industrial sectors, but we can expect new emerging sectors such as reconfigurable manufacturing, energy, and transport where these new possibilities can allow a rapid progress. The relative slowness of the removal processes in femtosecond mode is no longer a limitation and the unique quality of ultra-short processes is therefore accessible to an increasingly important panel of industrial implementation. The challenge of the thermal accumulation management is open in various application fields. Future development will use efficient and fast process development methods, using a loop that ultimately adjusts laser parameters to the process results. In this ambitious approach, the availability of a "smart" laser source allowing for an easier connection with the external environment is requested linked with the use of beam engineering tools, also connectable and controllable, in order to develop digital procedure for the process optimization.

Author contributions: All the authors have accepted responsibility for the entire content of this submitted manuscript and approved submission.
Research funding: None declared.
Conflict of interest statement: The authors declare no conflicts of interest regarding this article.

References

[1] J. Schille, L. Schneider, and U. Loeschner, "Process optimization in high-average-power ultrashort pulse laser microfabrication: how laser process parameters influence efficiency, throughput and quality," *Appl. Phys. A*, vol. 120, pp. 847–855, 2015.
[2] J. Lopez, K. Mishchik, G. Mincuzzi, E. Audouard, E. Mottay, and R. Kling, "Efficient metal processing using high average power ultrafast laser," *J. Laser MicroNanoeng.*, vol. 12, p. 3, 2017.
[3] J. Lopez, G. Mincuzzi, R. Devillard, et al., "Ablation efficiency of high-average power ultrafast laser,," *J. Laser Appl.*, vol. 27, p. S28008, 2015.
[4] P. Russbueldt, T. Mans, J. Weitenberg, H. D. Hoffmann, and R. Poprawe, "Compact diode-pumped 1.1 kW Yb:YAG Innoslab femtosecond amplifier," *Opt. Lett.*, vol. 35, pp. 4169–4171, 2010.
[5] C. Hönninger and E. Audouard, "Multi 100 W femtosecond laser perspectives," *LTJ*, vol. 2, pp. 50–53, 2018.
[6] B. Neuenschwander, B. Jaeggi, D. J. Foerster, T. Kramer, and S. Remund, "Influence of the burst mode onto the specific removal rate for metals and semiconductors," *J. Laser Appl.*, vol. 31, no. 2, p. 022203, 2019.
[7] T. Kramer, Y. Zhang, S. Remund, et al., "Increasing the specific removal rate for ultra short pulsed laser-micromachining by using pulse bursts," *J. Laser MicroNanoeng.*, vol. 12, pp. 107–114, 2017.

[8] J. Mur, L. Pirker, N. Osterman, and R. Petkovšek, "Silicon crystallinity control during laser direct microstructuring with bursts of picosecond pulses," *Opt. Express*, vol. 25, p. 26356, 2017.
[9] A. Žemaitis, P. Gečys, M. Barkauskas, G. Račiukaitis, and M. Gedvilas, "Highly-efficient laser ablation of copper by bursts of ultrashort tuneable (fs–ps) pulses," *Sci. Rep.*, vol. 9, p. 12280, 2019.
[10] D. J. Foerster, S. Faas, S. Gröninger, F. Bauer, A. Michalowski, and T. Graf, "Shielding effects and re-deposition of material during processing of metals with bursts of ultra-short laser pulses," *Appl. Surf. Sci.*, vol. 440, p. 926, 2018.
[11] C. Kerse, H. Kalaycioglu, P. Elahi, et al., "Ablation-cooled material removal with ultrafast bursts of pulses," *Nature*, vol. 537, p. 84, 2016.
[12] G. Bonamis, K. Mishchik, E. Audouard, et al., "Use of bursts up to GHz repetition rate for femtosecond ablation efficiency increase," *J. Laser Appl.*, vol. 31, p. 022205, 2019.
[13] K. Mishchik, G. Bonamis, J. Qiao, et al., "High-efficiency femtosecond ablation of silicon with GHz repetition rate laser source," *Opt. Lett.*, vol. 44, p. 2193, 2019.
[14] G. Bonamis, E. Audouard, C. Hönninger, et al., "Systematic study of laser ablation with GHz bursts of femtosecond pulses," *Opt. Express*, vol. 28, p. 27702, 2020.
[15] R. Marjoribanks, C. Dille, J. Schoenly, et al., "Ablation and thermal effects in treatment of hard and soft materials and biotissues using ultrafast-laser pulse-train bursts," *Photonics Laser Med.*, vol. 1, p. 155, 2012.
[16] J. Mur, J. Petelin, N. Osterman, and R. Petkovšek, "High precision laser direct microstructuring system based on bursts of picosecond pulses," *J. Phys. Appl. Phys.*, vol. 50, p. 325104, 2017.
[17] E. Audouard and E. Mottay, "Engineering model for ultrafast laser microprocessing," in *Frontiers in Ultrafast Optics: Biomedical, Scientific, and Industrial Applications XVI*, SPIE, 2016, p. 9740.
[18] F. Bauer, A. Michalowski, T. T. Kiedrowski, and S. Nolte, "Heat accumulation in ultra-short pulsed scanning laser ablation of metals," *Opt. Express*, vol. 23, p. 001035, 2015.
[19] A. Ancona, S. Döring, C. Jauregui, et al., "Femtosecond and picosecond laser drilling of metals at high repetition rates and average powers," *Opt. Lett.*, vol. 34, p. 3306, 2009.
[20] M. Domke, V. Matylitsky, and S. Stroj, "Surface ablation efficiency and quality of fs lasers in single-pulse mode, fs lasers in burst mode, and ns lasers," *Appl. Surf. Sci.*, vol. 505, p. 144594, 2020.
[21] P. Elahi, C. Akçaalan, C. Ertek, K. Eken, O. Ilday, and H. Kalaycoglu, "High power Yb-based all-fiber laser delivering 300 fs pulses for high speed ablation cooled material removal," *Opt. Lett.*, vol. 43, p. 535, 2018.
[22] L. Zhibin, H. Matsumoto, and J. Kleinert, *Ultrafast Laser Ablation of Copper with GHz-Bursts*, SPIE, 2018, pp. 10519–10521.
[23] C. Gaudiuso, G. Giannuzzi, A. Volpe, P. M. Lugarà, I. Choquet, and A. Ancona, "Incubation during laser ablation with bursts of femtosecond pulses with picosecond delays," *Opt. Express*, vol. 26, p. 3801, 2018.
[24] R. Ramaswami and K. Sivarajan, *Optical Networks: A Practical Perspective*, San Diego, CA, USA, Elsevier Science & Technology Books, 1998, OCLC: 892781758.
[25] A. Bartels, R. Cerna, C. Kistner, et al., "Ultrafast time-domain spectroscopy based on high-speed asynchronous optical sampling," *Rev. Sci. Instrum.*, vol. 78, p. 035107, 2007.
[26] A. Hatziefremidis, D. Papadopoulos, D. Fraser, and H. Avramopoulos, "Laser sources for polarized electron beams in CW and pulsed accelerators," *Nucl. Instrum. Methods Phys. Res. Sect. A Accel. Spectrom. Detect. Assoc. Equip.*, vol. 431, p. 4652, 1999.
[27] C. Kerse, H. H. Kalaycioglu, P. Elahi, N. Akçaalan, and F. M. Ilday, "3.5-GHz intra-burst repetition rate ultrafast Yb-doped fiber laser," *Opt. Commun.*, vol. 366, p. 404, 2016.
[28] A. Bartels, D. Heinecke, and S. A. Diddams, "Passively mode-locked 10 GHz femtosecond Ti:sapphire laser," *Opt. Lett.*, vol. 33, p. 1905, 2008.
[29] A. S. Mayer, C. R. Phillips, and U. Keller, "Watt-level 10-gigahertz solidstate laser enabled by self-defocusing nonlinearities in an aperiodically poled crystal," *Nat. Commun.*, vol. 8, p. 178, 2017.
[30] R. Paschotta, L. Krainer, S. Lecomte, et al., "Picosecond pulse sources with multi-GHz repetition rates and high output power," *New J. Phys.*, vol. 6, p. 174, 2004.
[31] A. Ishizawa, T. Nishikawa, A. Mizutori, et al., "Generation of 120-fs laser pulses at 1-GHz repetition rate derived from continuous wave laser diode," *Opt. Express*, vol. 19, p. 22402, 2011.
[32] A. Aubourg, J. Lhermite, S. Hocquet, E. Cormier, and G. Santarelli, "Generation of picosecond laser pulses at 1030 nm with gigahertz range continuously tunable repetition rate," *Opt. Lett.*, vol. 40, p. 5610, 2015.
[33] T. Hirsiger, M. Gafner, S. M. Remund, et al., "Machining metals and silicon with GHz bursts: surprising tremendous reduction of the specific removal rate for surface texturing applications," in *Proc. SPIE 11267, Laser Applications in Microelectronic and Optoelectronic Manufacturing (LAMOM) XXV*, 2020, p. 112670T, https://doi.org/10.1117/12.2543948.
[34] A. Žemaitis, M. Gaidys, P. Gečys, M. Barkauskas, and M. Gedvilas, "Femtosecond laser ablation by bibursts in the MHz and GHz pulse repetition rates," *Opt. Express*, vol. 29, p. 7641, 2021.
[35] S. Schwarz, S. Rung, C. Esen, and R. Hellmann, "Enhanced ablation efficiency using GHz bursts in micromachining fused silica," *Opt. Lett.*, vol. 46, p. 282, 2021.
[36] T. Menold, M. Ametowobla, J. R. Köhler, and J. H. Werner, "Surface patterning of monocrystalline silicon induced by spot laser melting," *J. Appl. Phys.*, vol. 24, p. 163104, 2018.
[37] J. Thorstensen and S. E. Foss, "Temperature dependent ablation threshold in silicon using ultrashort laser pulses," *J. Appl. Phys.*, vol. 112, p. 103514, 2012.
[38] C. Glassbrenner and G. A. Slack, "Thermal conductivity of silicon and germanium from 3 K to the melting point," *Phys. Rev.*, vol. 134, p. A1058, 1964.
[39] J. Bonse, K.-W. Brzezinka, and A. Meixner, "Modifying single-crystalline silicon by femtosecond laser pulses: an analysis by micro Raman spectroscopy, scanning laser microscopy and atomic force microscopy," *Appl. Surf. Sci.*, vol. 221, p. 215, 2004.

[40] G. Bonamis, E. Audouard, C. Hönninger, et al., Méthode de Détermination Des Conditions Opérationnelles d'un Procédé d'ablation Laser Femtoseconde à Très Haute Cadence Pour Un Matériau Donné, Patent n° 19 01188 (2019).
[41] L. L. Taylor, J. Qiao, and J. Qiao, "Optimization of femtosecond laser processing of silicon via numerical modeling," *Opt. Mater. Express*, vol. 6, p. 2745, 2016.
[42] M. E. Povarnitsyn, P. R. Levashov, and D. V. Knyazev, "Simulation of ultrafast bursts of subpicosecond pulses: in pursuit of efficiency," *Appl. Phys. Lett.*, vol. 112, p. 051603, 2018.
[43] G. Bonamis, *Conception et réalisation d'une source laser femtoseconde GHz et applications au régime d'ablation très haute cadence*, Université de Bordeaux, 2020. https://www.theses.fr/2020BORD0293.
[44] J. Schille, L. Schneider, P. Lickschat, U. Loeschner, R. Ebert, and H. Exner, "High-pulse repetition frequency ultrashort pulse laser processing of copper," *J. Laser Appl.*, vol. 27, p. S28007, 2015.
[45] F. Nyenhuis, A. Michalowski, and J. A. L'Huillier, "Surface treatment with GHz-bursts," in *Proc. SPIE 11268, Laser-Based Micro- and Nanoprocessing*, vol. XIV, 2020, p. 112680B.
[46] D. Metzner, P. Lickschat, and S. Weiÿmantel, "High-quality surface treatment using GHz burst mode with tunable ultrashort pulses," *Appl. Surf. Sci.*, vol. 531, p. 147270, 2020.
[47] D. J. Forster, B. Jaggi, A. Michalowski, and B. Neuenschwander, "Review on experimental and theoretical investigations of ultra short pulse laser ablation of metals with burst pulses," *Materials*, vol. 14, p. 3331, 2021.
[48] T. Tamaki, W. Watanabe, J. Nishii, and K. Itoh, "Welding of transparent materials using femtosecond laser pulses," *Jpn. J. Appl. Phys.*, vol. 44, p. L687, 2005.
[49] Y. Ozeki, T. Inoue, T. Tamaki, et al., "Direct welding between copper and glass substrates with femtosecond laser pulses," *APEX*, vol. 1, p. 082601, 2008.
[50] H. Penilla, L. F. Devia-Cruz, A. T. Wieg, et al., "Ultrafast laser welding of ceramics," *Science*, vol. 365, pp. 803–808, 2019.
[51] M. Chambonneau, Q. Li, V. Fedorov, M. Blothe, S. Tzortzakis, and S. Nolte, "Semiconductor-metal ultrafast laser welding with relocated filaments," in *Proc. SPIE 11676, Frontiers in Ultrafast Optics: Biomedical, Scientific, and Industrial Applications*, vol. XXI, p. 1167610, 2021.